JACS
JOURNAL OF THE AMERICAN CHEMICAL SOCIETY

ARTICLE

pubs.acs.org/JACS

Binaphthol-Derived Bisphosphoric Acids Serve as Efficient Organocatalysts for Highly Enantioselective 1,3-Dipolar Cycloaddition of Azomethine Ylides to Electron-Deficient Olefins

Long He,[†,‡] Xiao-Hua Chen,[†] De-Nan Wang,[†] Shi-Wei Luo,[*,†] Wen-Quan Zhang,[†] Jie Yu,[†] Lei Ren,[†] and Liu-Zhu Gong[*,†]

[†]Hefei National Laboratory for Physical Sciences at the Microscale and Department of Chemistry, University of Science and Technology of China, Hefei, 230026, China

[‡]College of Chemistry and Chemical Engineering, China West Normal University, Nanchong, 637002, China

Supporting Information

ABSTRACT: A variety of chiral bisphosphoric acids derived from binaphthols have been evaluated for enantioselective 1,3-dipolar cycloaddition reactions, revealing that the feature of the linker in the catalysts exerted great impact on the stereoselectivity. Among them, the oxygen-linked bisphosphoric acid **1a** provided the highest level of stereoselectivity for the 1,3-dipolar cycloaddition reaction tolerating a wide range of substrates including azomethine ylides, generated *in situ* from a broad scope of aldehydes and α-amino esters, and various electron-deficient dipolarophiles such as maleates, fumarates, vinyl ketones, and esters. This reaction actually represents one of the most enantioselective catalytic approaches to access structurally diverse pyrrolidines with excellent optical purity. Theoretical calculations with DFT method on the formation of azomethine ylides and on the transition states of the 1,3-dipolar cycloaddition step showed that the dipole and dipolarophile were simultaneously activated by the bifunctional chiral bisphosphoric acids through the formation of hydrogen bonds. The effect of the bisphosphoric acids on reactivity and stereochemistry of the three-component 1,3-dipolar cycloaddition reaction was also theoretically rationalized. The bisphosphoric acid catalyst **1a** may take on a half-moon shape with the two phosphoric acid groups forming two intramolecular hydrogen bonds. In the case of maleates, one phosphate acts as a base to activate the 1,3-dipole, and simultaneously, the two hydroxyl groups in the catalyst **1a** may respectively form two hydrogen bonds with the two ester groups of maleate to make it more electronically deficient as a much stronger dipolarophile to participate in a concerted 1,3-dipolar cycloaddition with azomethine ylide. However, in the cases involving acrylate and fumarate dipolarophiles, only one hydroxyl group forms a hydrogen bond with the ester functional group to lower the LUMO of the C−C double bond and another one is remained to adjust the acidity and basicity of two phosphoric acids to activate the dipole and dipolarophile more effectively.

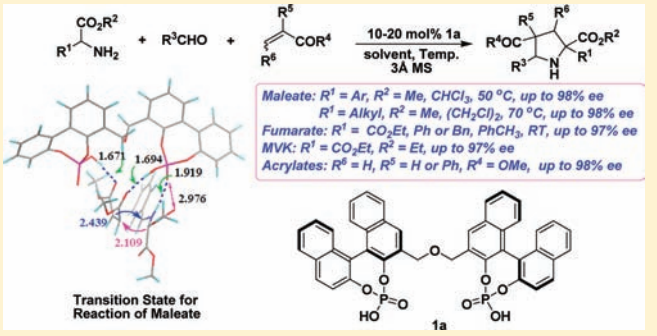

INTRODUCTION

The rapid and facile construction of structurally diverse heterocycles in enantiomerically pure form is among the most important tasks in medically relevant fields, particularly in chemical biology.[1] Five-membered nitrogenous heterocycles, in particular, pyrrolidines actually occupy a privileged position in organic chemistry, because they are key structural motifs prevalent in numerous natural alkaloids as exemplified by the molecules shown in Figure 1, and in biologically active unnatural substances. Moreover, they also served as the chiral building blocks or intermediates in the synthesis of natural alkaloids and medicinally relevant compounds.[2] Consequently, the development of efficient methods to access optically pure pyrrolidine skeletons are undoubtedly appealing in the organic synthesis.

The 1,3-dipolar cycloaddition reaction of azomethine ylides with electronically poor olefins represents one of the most efficient synthetic methods to access pyrolidine structural motifs.[3] Auxiliary-controlled 1,3-dipolar cycloaddition has been a reliable method to produce optically pure pyrrolidine structural motifs by using either the optically pure azomethine ylides or dipolarophiles.[4] Allway and Grigg first demonstrated that stoichiometric amounts of chiral cobalt, manganese, and silver complexes were able to promote the 1,3-dipolar cycloaddition reactions of azomethine ylides derived from arylidene imines of glycine with high enantioselectivity.[5] The first catalytic enantioselective 1,3-dipolar cycloaddition reaction of azomethine ylides was established independently by Zhang[6a] and Jørgensen[6b] who respectively exploited chiral silver and copper catalysts to accelerate the reaction and control the stereochemistry. After these two events, tremendous efforts have been directed toward the design of new catalysts or ligands applicable to controlling

Received: May 7, 2011
Published: July 22, 2011

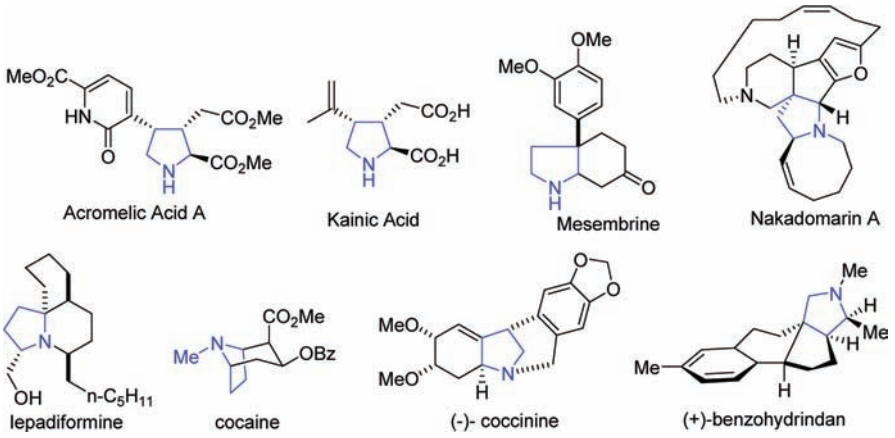

Figure 1. Naturally occurring alkaloids contain pyrrolidine motifs.

stereoselectivity in 1,3-dipolar cycloaddition reactions involving azomethine ylides. As a result, many privileged bidentate ligands turned out to give high levels of enantioselectivity over the last decades.[7] However, Lewis acid-catalyzed 1,3-dipolar cycloaddition reactions are mostly sensitive to the substrates and usually one chiral ligand or catalyst is highly enantioselective for one specific type of dipolarophiles. Therefore, structurally diverse chiral ligands are basically required to realize highly stereoselective 1,3-dipolar cycloaddition reactions for different types of dipolarophiles, and thereby somewhat hindering the practical use. In addition, a catalytic amount of external base is used for the generation of azomethine ylides. In recent years, organocatalytic 1,3-dipolar cycloaddition reactions of azomethine ylides to dipolarophiles have been discovered. α-Amino acids have found their applications to the catalytic 1,3-dipolar cycloaddition of azomethine ylides to electron-deficient olefins, but with a very low enantioselectivity (up to 12% ee).[8] The enones and enals activated by lowering the LUMO through the formation of iminium intermediates with chiral secondary amine catalysts proved to be highly reactive toward the azomethine ylides in high stereoselectivity. However, this process only works for the substrates capable of forming unsaturated iminium species with amine and therefore is principally limited to enal and enone dipolarophiles.[9] On the other hand, both nitroolefins and imino esters could be simultaneously activated by bifunctional thiourea catalysts to undergo a formal [3 + 2] cycloaddition with stereocontrol.[10] However, only nitroolefins have been reported to be reactive substrates in this reaction. Yamamoto has demonstrated that chiral *N*-triflyl phosphoramide is used for an asymmetric 1,3-dipolar cycloaddition of diaryl nitrones to ethyl vinyl ether to give the endo products in high ee's (up to 93% ee).[11] Herein, we will present a three-component 1,3-dipolar cycloaddition of azomethine ylides with electron-deficient olefins, which provided high levels of enantioselectivity for a wide range of substrates including azomethines, generated *in situ* from a wide scope of aldehydes and α-amino esters, and different types of electron-deficient dipolarophiles such as maleates, fumarates, vinyl ketones, and acrylates. In addition, a detailed theoretical investigation on the reaction mechanism will also be reported.[12]

■ INITIAL CONSIDERATION OF THE BRØNSTED ACID-CATALYZED THREE-COMPONENT REACTION AND SUMMARY OF PRELIMINARY RESULTS

Binol-derived phosphoric acids containing a strong acidic hydroxyl and a Lewis basic phosphoryl oxygen have been proven to be privileged bifunctional catalysts broadly applicable to afford a large number of highly enantioselective organic transformations.[13] Initially, we envisioned that the bifunctional phosphoric acid is theoretically able to form a chiral azomethine ylide dipole **IIa** or **IIb** with an azomethine compound through double hydrogen bonds. These chiral azomethine ylides were presumably reactive toward electron deficient olefins to undergo the 1,3-dipolar cycloaddition reaction in enantioselective manner (eq 1).

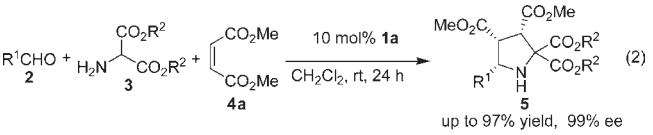

Following up this consideration, we carried out the three-component 1,3-dipolar cycloaddition reaction of 4-nitrobenzaldehyde (**2a**) with diethyl amino malonate (**3a**) and dimethyl maleate (**4a**) in the presence of a chiral phosphoric acid and found that the binol-derived phosphoric acids are able to catalyze the reaction and a bisphosphoric acid **1a** was identified as the catalyst of choice, conferring exquisite levels of stereoselectivity for the reaction capable of accommodating a wide scope of aldehydes (eq 2).[12] Subsequent studies found that the bisphosphoric acid was also amenable to the 1,3-dipolar cycloaddition of 2,3-allenoates with stereochemical control, yielding 3-methylenepyrrolidine derivatives with excellent enantioselectivity.[14] Additionally, on the basis of this general strategy, we established a three-component 1,3-dipolar cycloaddition reaction of methyleneindolinones with azomethine ylides catalyzed by a 3,3′-di-(2-naphthyl) binol-based phosphoric acid, offering a facile entry to spiro [pyrrolidin-3,3′-oxindole] derivatives with high enantioselectivity and structural diversity.[15] Theoretical calculations on this reaction suggested that both the azomethine ylide and the methyleneindolinone are simultaneously activated by hydrogen-bonds with the phosphoryl oxygen and hydroxyl of the

dx.doi.org/10.1021/ja204218h |*J. Am. Chem. Soc.* 2011, 133, 13504–13518

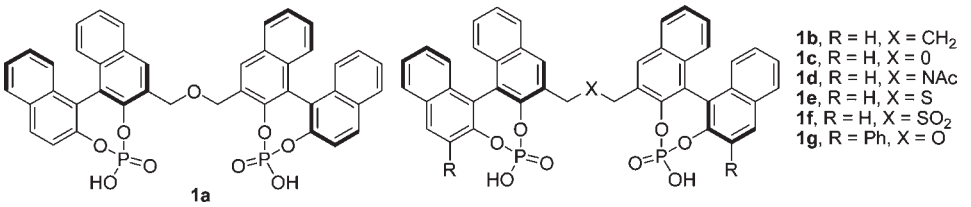

Figure 2. Bisphosphoric acids evaluated in this study.

phosphoric acid, respectively, to afford a stereocontrolled 1,3-dipolar cycloaddition.[15] Despite these findings, however, some issues related with the 1,3-dipolar cycloaddition reaction catalyzed by the bisphosphoric acid remain including that (1) the effect of the feature of the linker in bisphosphoric acids on the reaction should be clarified; (2) detailed mechanistic studies to understand why this bisphosphoric acid is more stereoselective than mono ones have not been conducted; and (3) the generality for the dipolarophiles other than maleates has not been explored. Thus, this article will be focused on detailed studies on the reaction catalyzed by the bisphosphoric acids (**1a**−**1g**) bearing different linkers to address the issues mentioned above (Figure 2).

RESULTS AND DISCUSSION

The Preparation of Bisphosphoric Acids. The bisphosphoric acid catalysts **1a**−**1g** were prepared starting with BINOL, which were first transformed into tetraols bearing various linkers referring to known reaction procedures established by Shibasaki[16] and others,[17] and followed by a reaction with 4 equiv of phosphorus oxychloride in the presence of pyridine and a subsequent hydrolysis under acidic conditions. The synthetic details have been shown in the Supporting Information.

The 1,3-Dipolar Cycloaddition of 4-Nitrobenzaldehyde with Diethyl Aminomalonate and Dimethyl Maleate Catalyzed by Different Bisphosphoric Acids. Our previous evaluation of binol-based phosphoric acids found that the bisphosphoric acid **1a** was the most effective and stereoselective chiral catalyst for the three-component 1,3-dipolar cycloaddition reaction of aldehydes with diethyl amino malonate and dimethyl maleate, whereas the monophosphoric acids only delivered moderate stereoselectivity.[12] Moreover, the α-phenylglycine methyl ester also participated in the reaction but at an elevated temperature (50 °C). These preliminary results drew our attention to investigate the correlation between the structure of bisphosphoric acids and reaction performance to seek the optimal reaction conditions for the highly enantioselective 1,3-dipoar cycloaddition reaction tolerating different substrates. Thus, we reinvestigated the reaction of 4-nitrobenzaldhyde (**2a**) with diethyl aminomalonate (**3a**) and dimethyl maleate (**4a**) in dichloromethane at room temperature in the presence of 10 mol % of bisphosphoric acids **1a**−**g**. Interestingly, the linker in the bisphosphoric acids exerts great impact on the control of stereoselectivity (Table 1). The replacement of the oxygen with methylene led to a catalyst **1b**, which provided a dramatically reduced catalytic activity although the enantioselectivity eroded slightly (entry 1 vs 2). The two carbon-bridged bisphosphoric acid **1c** gave moderate yield with low enantioselectivity (entry 3). The incorporation of heteroatoms other than oxygen into the linker resulted in a poor enantioselectivity (entries 4−6). In particular, the sulfonyl bridged bisphosphoric acid **1f** showed poor catalytic activity albeit with a moderate enantioselectivity (entry 6). The

Table 1. Evaluation of the Bisphosphoric Acids[a]

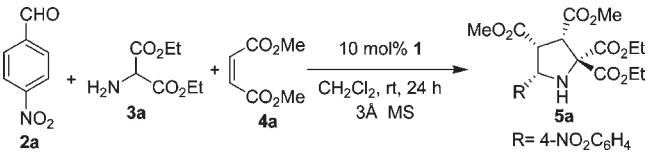

entry	1	yield (%)[b]	ee (%)[c]
1	**1a**	96	98
2	**1b**	33	92
3	**1c**	79	45
4	**1d**	27	10
5	**1e**	74	23
6	**1f**	26	76
7	**1g**	50	59
8	**1a**	89	96[d]

[a] The reaction was performed in 0.1 mmol scale. [b] Isolated yield and a single diastereomer was observed unless indicated otherwise. [c] The ee was determined by HPLC. [d] **1a** was twice subjected to a short-path column chromatography using extra pure silica gel (Merck) after washing with HCl (2 M).

introduction of phenyl substituents to the bisphosphoric acid, as shown in **1g**, led to a much lower catalytic efficacy and stereocontrolling ability in comparison with **1a** (entry 7 vs 1). The use of acid washed **1a**, which was twice subjected to a short-path column chromatography using extra pure silica gel, gave a comparable yield and enantioselectivity (entry 8). These results in combination with the control reaction catalyzed by calcium salt of **1a** suggested that no metal contamination affected the stereoselectivity.[18]

The 1,3-Dipolar Cycloaddition of 4-Nitrobenzaldehyde with Diethyl Aminomalonate and Either 3-Butenone or Methyl Acrylate Catalyzed by Bisphosphoric Acid 1a. Besides the substrates examined in the preliminary report,[12] additional investigations were performed on the generality of the protocol for vinyl ketones and acrylate esters (Table 2). Although acrylate esters were previously investigated as dipolarophiles in the metal complex-catalyzed asymmetric 1,3-dipolar cycloadditions, high levels of enantioselectivity were only observed for the *tert*-butyl acrylate[7a,b,19] with exception of protocols reported by Kobayashi[7f,g] and Wang.[7h] Moreover, 2-substituted acrylate esters, which undergo the dipolar cycloaddition to give pyrrolidines bearing an all-carbon stereogenic center, and methyl vinyl ketone (MVK) have not been explored as dipolarophiles, yet. Delightedly, the methyl vinyl ketone was well tolerated and participated in smoothly phosphoric acid-catalyzed 1,3-dipolar cycloaddition reactions with various aldehydes, producing the pyrrolidine derivatives with high enantioselectivities ranging from 86% to 97% ee (entries 1−9). Interestingly, methyl acrylate also engaged

Table 2. Scope of Aldehydes in the Asymmetric Three-Component 1,3-Dipolar Cycloaddition Reaction Involving Diethyl α-Aminomalonate with Vinyl Ketones and Esters[a]

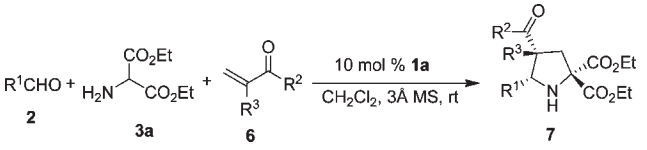

entry	7	R^1	R^2	R^3	time (h)	yield (%)[b]	ee (%)[c]
1	**7a**	4-$NO_2C_6H_4$	CH_3	H	48	77	96[d]
2	**7b**	4-CNC_6H_4	CH_3	H	74	47	96
3	**7c**	4-$MeO_2CC_6H_4$	CH_3	H	72	51	87[e]
4	**7d**	4-BrC_6H_4	CH_3	H	72	58	95
5	**7e**	4-ClC_6H_4	CH_3	H	74	64	91
6	**7f**	4-FC_6H_4	CH_3	H	72	43	94
7	**7g**	2-$NO_2C_6H_4$	CH_3	H	64	85	96[d]
8	**7h**	3-ClC_6H_4	CH_3	H	70	43	86(96)[f,g]
9	**7i**	3-$NO_2C_6H_4$	CH_3	H	74	63	97[d]
10	**7j**	4-$NO_2C_6H_4$	OCH_3	H	48	82	95
11	**7k**	2-$NO_2C_6H_4$	OCH_3	H	72	91	92
12	**7l**	4-CNC_6H_4	OCH_3	H	64	96	96
13	**7m**	3-$NO_2C_6H_4$	OCH_3	H	48	84	97[e]
14	**7n**	4-BrC_6H_4	OCH_3	H	64	80	97
15	**7o**	4-$MeO_2CC_6H_4$	OCH_3	H	48	79	84
16	**7p**	4-$NO_2C_6H_4$	OCH_3	Ph	48	85	94[d]
17	**7q**	4-BrC_6H_4	OCH_3	Ph	72	85	97[d]
18	**7r**	4-ClC_6H_4	OCH_3	Ph	72	65	94[f]
19	**7s**	4-CNC_6H_4	OCH_3	Ph	72	71	96[d]
20	**7t**	2-$NO_2C_6H_4$	OCH_3	Ph	60	85	98[f]

[a] The reaction was carried out in 0.1 mmol scale in dichloromethane (1 mL) with 3 Å MS (150 mg), and the ratio of **2**/**3a**/**6** was 1.2/1/5. [b] Isolated yield and a single diastereomer was observed unless indicated otherwise. [c] The ee values were determined by HPLC analysis. [d] >99/1 *dr*. [e] 99/1 *dr*. [f] 98/2 *dr*. [g] After a single recrystallization from ethyl acetate.

in the reaction to give high yields and excellent enantioselectivities (entries 10−15, 84−97% ee). More importantly, methyl 2-phenylacrylate underwent the three-component 1,3-dipolar cycloaddition reaction with a variety of aldehydes and aminomalonate to furnish pyrrolidine derivatives possessing an all-carbon quaternary stereogenic center in good yields (65−85%) and with excellent enantioselectivities (entries 16−20, 94−98% ee).[20] The configurations of the products were assigned to be (4*R*, 5*S*) by X-ray analysis of **7 h** (Figure 3).

The 1,3-Dipolar Cycloaddition of Aldehydes with Maleates and Diethyl α-Amino Esters. However, the extension of the reaction conditions to α-phenylglycine methyl ester failed to undergo the 1,3-dipolar cycloaddition reaction (Table 3, entry 1). Encouragingly, the reaction proceeded at elevated temperature (50 °C) in chloroform to give the desired product in a high yield and with an excellent enantioselectivity (entry 2).[12] Interestingly, all carbon-bridged bisphosphoric acid **1b** was also able to offer excellent enantioselectivity (entry 4). In terms of the efficiency and stereochemical control, **1a** is still the catalyst of choice. The presence of 20 mol % of **1a** ensured a clean reaction in 92% yield and with 97% ee (entry 3).

With the optimal conditions in hand, we explored the generality of the protocol for other different aldehydes and

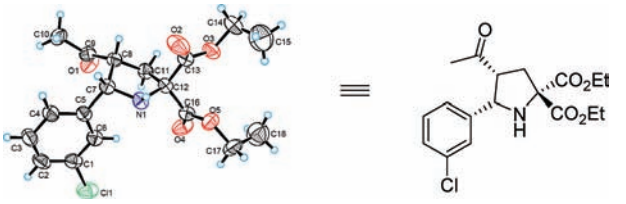

Figure 3. X-ray structure of **7h** .

Table 3. Optimization of Conditions for the Reaction Involving α-Phenylglycine Methyl Ester[a]

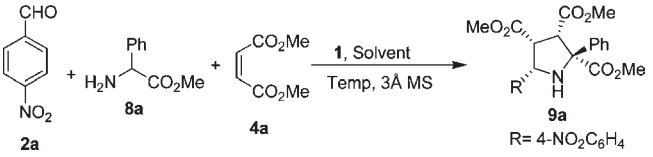

entry	**1** (mol %)	solvent	temp. (°C)	yield (%)[b]	ee (%)[c]
1	**1a** (10)	CH_2Cl_2	RT	trace	–
2	**1a** (10)	$CHCl_3$	50	55	97
3	**1a** (20)	$CHCl_3$	50	92	97
4	**1b** (20)	$CHCl_3$	50	78	98

[a] The reaction was carried out in 0.2 mmol scale in a solvent (2 mL) with 3 Å MS (300 mg) for 48 h, and the ratio of **2a**/**8a**/**4a** was 5/4/1. [b] Isolated yield and a single diastereomer was observed unless indicated otherwise. [c] The ee values were determined by HPLC analysis.

α-phenylglycine ester derivatives (Table 4). A wide scope of aldehydes including aromatic, aliphatic, and unsaturated variants were able to participate in the reaction. *para*-Substituted benzaldehydes underwent the 1,3-dipolar cycloaddition in excellent yields and with high enantioselectivities ranging from 87 to 97% ee (entries 1−6). *meta*-Nitro and cyanobenzaldehydes provided 96% and 92% ee's, respectively, but a lower yield was obtained for the cyanobenzaldehyde (entries 7 and 8). Interestingly, the stereochemical outcomes are to some degree reliant on the electronic properties of the *ortho*-substituents on benzaldehydes and benefit from the electron-withdrawing group. For instance, the highest ee value was found in the reaction of 2-nitrobenzaldehyde (entry 9) while comparably lower enantioselectivities ranging from 83% to 91% ee were delivered to 2-haleganated benzaldehydes (entries 10−12). Disubstituted benzaldehydes were also suitable reaction components and participated in clean reactions with 88−98% ee (entries 13−15). In contrast, aliphatic aldehydes proved to be less reactive and gave much lower enantiomeric excesses (entries 16 and 17). Cinnamaldehyde derivatives were accommodated to give desired products in high yields (96% and 89%, respectively) and with excellent stereoselectivities (96% and 98% ee, respectively, entries 18 and 19). Although phenylpropiolaldehyde was a good reaction partner, a moderate enantioselectivity was obtained (entry 20). Variation of the ester pattern on either α-amino esters (**8**) or maleates (**4**) led to very little change in the reaction conversion and the stereoselectivity (entries 21 and 22). The configuration of **9e** (R^1 = 4-BrC_6H_4) was assigned to be (2*S*,3*S*,4*R*,5*S*) by X-ray analysis (Figure 4).

Additionally, the generality for α-arylglycine methyl esters other than methyl α-phenylglycine was explored (Table 5). The substitution on the benzene ring was well tolerated to give a clean

Table 4. Scope of Aldehydes in the Asymmetric Three-Component 1,3-Dipolar Cycloaddition Reaction Involving α-Phenylglycine Esters[a]

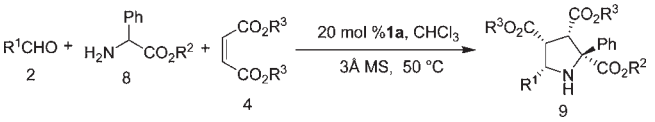

entry	9	R_1	R_2	R_3	yield (%)[b]	ee (%)[c]
1	**9b**	4-$CF_3C_6H_4$	CH_3	CH_3	98	94
2	**9c**	C_6H_5	CH_3	CH_3	90	89
3	**9d**	4-CNC_6H_4	CH_3	CH_3	96	87
4	**9e**	4-BrC_6H_4	CH_3	CH_3	93	97
5	**9f**	4-ClC_6H_4	CH_3	CH_3	96	94
6	**9g**	4-FC_6H_4	CH_3	CH_3	86	94
7	**9h**	3-$NO_2C_6H_4$	CH_3	CH_3	86	96
8	**9i**	3-CNC_6H_4	CH_3	CH_3	65	92
9	**9j**	2-$NO_2C_6H_4$	CH_3	CH_3	98	96
10	**9k**	2-FC_6H_4	CH_3	CH_3	96	87
11	**9l**	2-ClC_6H_4	CH_3	CH_3	95	83
12	**9m**	2-BrC_6H_4	CH_3	CH_3	96	91
13	**9n**	2-Cl,4-FC_6H_3	CH_3	CH_3	94	96
14	**9o**	3-Cl,4-FC_6H_3	CH_3	CH_3	87	88
15	**9p**	4-Cl,3-FC_6H_3	CH_3	CH_3	84	98
16	**9q**	c-C_6H_{11}	CH_3	CH_3	58	75
17	**9r**	c-C_3H_5	CH_3	CH_3	61	74
18	**9s**	4-$MeOC_6H_4CH{=}CH$	CH_3	CH_3	96	96
19	**9t**	4-$NO_2C_6H_4CH{=}CH$	CH_3	CH_3	89	98
20	**9u**	$PhC{\equiv}C$	CH_3	CH_3	83	78
21	**9v**	4-$NO_2C_6H_4$	CH_3	C_2H_5	95	92
22	**9w**	4-$NO_2C_6H_4$	C_2H_5	CH_3	95	95

[a] The reaction was carried out in 0.2 mmol scale in chloroform (2 mL) with 3 Å MS (300 mg) for 48−72 h and the ratio of **2**/**8**/**4** was 5/4/1. However, a messy reaction was observed for *n*-alkyl aldehydes and *tert*-butyl aldehyde did not participate in the 1,3-dipolar cycloaddition. [b] Isolated yield and a single diastereomer was observed unless indicated otherwise. [c] The ee values were determined by HPLC analysis.

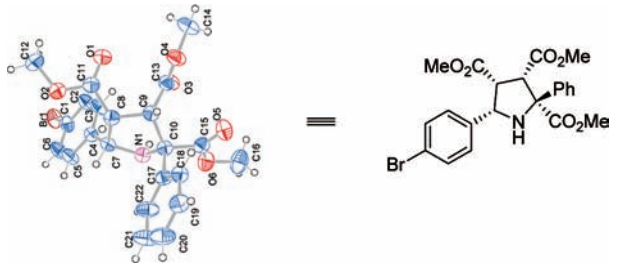

Figure 4. The X-ray structure of **9e**.

cycloaddition reaction with excellent enantioselectivities regardless of the electronic feature and the position of the substituents (94−98% ee, entries 1−8). The reaction involving a disubstituted phenylglycine methyl ester occurred with a high stereoselectivity as exemplified by 3-chloro-4-methoxyphenyl glycine methyl ester (91% ee, entry 9).

However, the further application of the optimized conditions to the reaction involving racemic methyl phenylalanine led to an incomplete reaction albeit with a high enantioselectivity of 94% ee, presumably due to the lower reactivity in comparison with the α-aryl analogues (Table 6, entry 1). Thus, the reaction conditions were reoptimized to improve the efficiency. Screening of reaction parameters including solvents and temperature elucidated that the best results in terms of both the yield and stereoselectivity were achieved when the reaction was conducted in 1,2-dichloroethane at 70 °C by using 20 mol % of **1a** (entry 2).

The reoptimized conditions were then applied to structurally different α-alkyl amino esters (Table 7). Among the methyl phenylalanine derivatives, the substituent on the phenyl group exerted very little impact on the stereoselectivity. The substitution of the phenylalanine with either electron-withdrawing or donating group was tolerated with exquisite enantioselectivities ranging from 97% to 98% ee (entries 1−8). Interestingly, methyl α-aminobutyrate also participated in the 1,3-dipolar

Table 5. Scope of α-Arylglycine Methyl Esters[a]

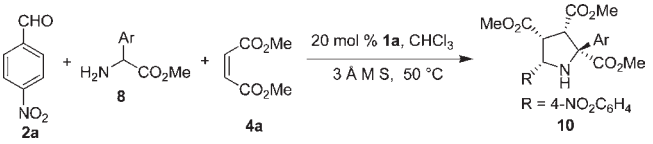

entry	10	Ar	time (h)	yield (%)[b]	ee (%)[c]
1	**10a**	4-ClC_6H_4	60	96	97
2	**10b**	3-ClC_6H_4	54	96	94
3	**10c**	2-ClC_6H_4	54	95	98
4	**10d**	4-FC_6H_4	60	94	95
5	**10e**	3-FC_6H_4	64	93	95
6	**10f**	2-FC_6H_4	48	96	98
7	**10g**	4-$MeOC_6H_4$	50	91	96
8	**10h**	4-$MeO_2CC_6H_4$	52	97	95
9	**10i**	3-Cl, 4-$MeOC_6H_3$	48	92	91

[a] The reaction was carried out in 0.2 mmol scale in chloroform (2 mL) with 3 Å MS (300 mg), and the ratio of **2a**/**8**/**4a** was 5/4/1. [b] Isolated yield and a single diastereomer was observed unless indicated otherwise. [c] The enantiomeric excesses were determined by HPLC analysis.

Table 6. Optimization of Reaction Conditions of the Asymmetric Three-Component 1,3-Dipolar Cycloaddition Reactions Involving Methyl Phenylalanine[a]

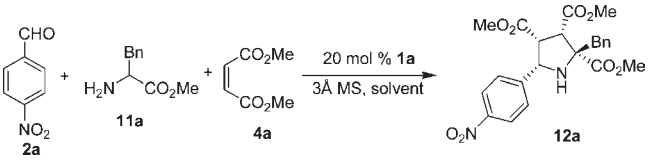

entry	temp (°C)	solvent	yield (%)[b]	ee (%)[c]
1	50	$CHCl_3$	30	94
2	**70**	**$ClCH_2CH_2Cl$**	**88**	**98**
3	70	$PhCH_3$	84	96

[a] The reaction was carried out in 0.2 mmol scale in solvent (2 mL) with 3 Å MS (300 mg) for 48 h, and the ratio of **2a**/**11a**/**4a** was 5/4/1. [b] Isolated yield and a single diastereomer was observed unless indicated otherwise. [c] The enantiomeric excesses were determined by HPLC analysis.

Table 7. Scope of Phenylalanine Esters in the Asymmetric Three-Component 1,3-Dipolar Cycloaddition Reactions[a]

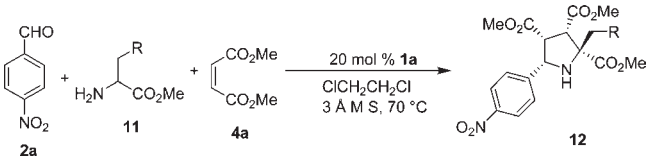

entry	12	R	time (h)	yield (%)[b]	ee (%)[c]
1	**12a**	Ph	60	88	98
2	**12b**	4-ClC_6H_4	48	82	96
3	**12c**	4-BrC_6H_4	48	88	97
4	**12d**	2-FC_6H_4	48	92	98
5	**12e**	4-$MeOC_6H_4$	48	92	98
6	**12f**	4-$CH_3CO_2C_6H_4$	50	81	98
7	**12g**	4-FC_6H_4	42	65	97
8	**12h**	3-FC_6H_4	46	73	98
9	**12i**	Me	72	79	94

[a] The reaction was carried out in 0.2 mmol scale in 1, 2-dichloroethane (2 mL) with 3 Å MS (300 mg), and the ratio of **2a**/**11**/**4a** was 5/4/1. [b] Isolated yield and a single diastereomer was observed unless indicated otherwise. [c] The ee values were determined by HPLC analysis.

Table 8. Optimization of Reaction Conditions for Dimethyl Fumarate[a]

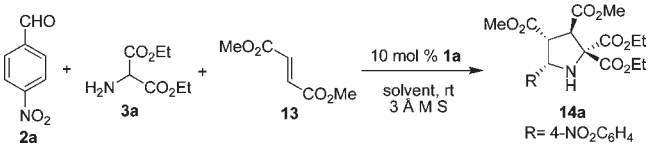

entry	solvent	yield (%)[b]	endo/exo[c]	ee (%)[d]
1	CH_2Cl_2	92	2/1	**73**
2	$CHCl_3$	71	7.5/1	96
3	$ClCH_2CH_2Cl$	82	8/1	95
4	THF	38	1/2	10
5	CH_3CN	78	1/1	40
6	$PhCH_3$	82	8.5/1	**97**

[a] The reaction was carried out in 0.1 mmol scale in solvent (1 mL) with 3 Å MS (150 mg) at 25 °C for 24 h, and the ratio of **2a**/**3a**/**13** was **1.2**/**1**/**5**. [b] Isolated yield. [c] Determined by ^{1}H NMR. [d] The ee values were determined by HPLC analysis.

cycloaddition in a good conversion and with excellent enantioselectivity although a prolonged time was required (entry 9).

The 1,3-Dipolar Cycloaddition of Fumarate with Diethyl Aminomalonate and Aldehydes. In comparison with maleates, fumarates represent challenging dipolarophiles in the asymmetric 1,3-dipolar cycloaddition reaction. Jørgensen and coworkers accomplished a successful 1,3-dipolar cycloaddition reaction of fumarates with azomethine ylides using a zinc complex of *tert*-BOX ligand while the highest level of enantioselectivity reached 90% ee.[6b] When we applied the optimal conditions to the 1,3-dipolar cycloaddition involving dimethyl maleate to dimethyl fumarate, the reaction proceeded smoothly to give the cycloadduct in a high yield but with a moderate enantioselectivity and a low diastereoselectivity (Table 8, entry 1). Screening of

Table 9. Generality for Amino Esters and Aldehydes[a]

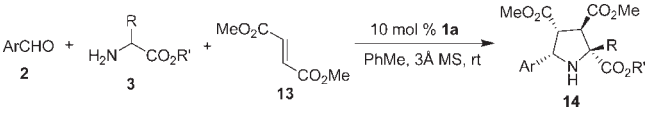

entry	14	Ar	R	R′	yield (%)[b]	endo/exo[c]	ee (%)[d]
1	**14b**	4-BrC_6H_4	CO_2Et	Et	89	10/1	95
2	**14c**	4-ClC_6H_4	CO_2Et	Et	77	9/1	91(22)
3	**14d**	4-CNC_6H_4	CO_2Et	Et	83	8/1	96(47)
4	**14e**	3-$NO_2C_6H_4$	CO_2Et	Et	80	9.5/1	97(23)
5	**14f**	2-$NO_2C_6H_4$	CO_2Et	Et	93	8/1	92
6	**14g**	4-$NO_2C_6H_4$	Ph	Et	99	3.8/1	97[e] (10)
7	**14h**	4-$NO_2C_6H_4$	Bn	Me	99	4/1	50[f] (2)

[a] The reaction was carried out in 0.1 mmol scale in toluene (1 mL) with 3 Å MS (150 mg) at 25 °C for 24−48 h, and the ratio of **2a**/**3**/**13** was 1.2/1/5. [b] Isolated yield. [c] Determined by ^{1}H NMR. [d] The ee values were determined by HPLC analysis and the ee in parentheses is for the minor diastereomer. [e] at 50 °C. [f] At 70 °C.

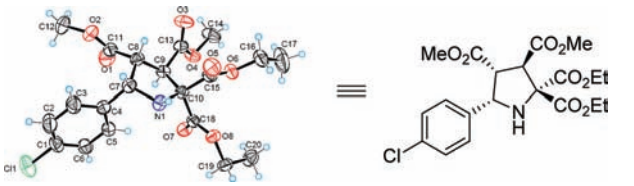

Figure 5. X-ray structure of **14c**..

solvents found that chloroform and 1,2-dichloroethane could deliver high enantioselectivities of 96% and 95% ee, respectively (entries 2 and 3), whereas poor stereoselectivities were observed in THF and acetonitrile (entries 4 and 5). Delightedly, the best results in terms of reaction efficiency and stereoselectivity were attained by conducting the reaction in toluene (entry 6).

With the optimal conditions for the 1,3-dipolar cycloaddition of dimethyl fumarate in hand, we explored the generality for the aldehydes and amino esters (Table 9). The substitution of benzaldehyde derivatives with electron-withdrawing group at either the *para*- or *meta*-position was well operative in the 1,3-dipolar cycloaddition with dimethyl fumarate (**13**), leading to highly substituted pyrrolidine derivatives in high yields and with good diastereomeric ratios and excellent ee values (entries 1−5). More interestingly, the ethyl α-phenylglycine gave a quantitative yield and excellent enantioselectivity, but the diastereomeric ratio was unsatisfactory (entry 6). However, a moderate enantioselectivity was obtained in the case involving methyl phenylalanine (entry 7). The absolute configuration was assigned to (3*R*,4*R*,5*S*) by X-ray analysis of **14c** (Figure 5).

Computational Studies on the Reaction Mechanism by DFT Calculation. The BINOL-derived phosphoric acid catalysts acted simultaneously as an acid and a base to activate both the nucleophile and electrophile in many reaction mechanisms.[21] To gain deeper insight into this asymmetric 1,3-dipolar cycloaddition reaction involving BINOL-derived bisphosphoric acid catalysts, full DFT calculations were performed. The B3LYP functional[22] combined with the 6-31G(d) basis set,[23] as implemented in the Gaussian03 program,[24] was used for geometry optimization of all intermediates and transition state structures.

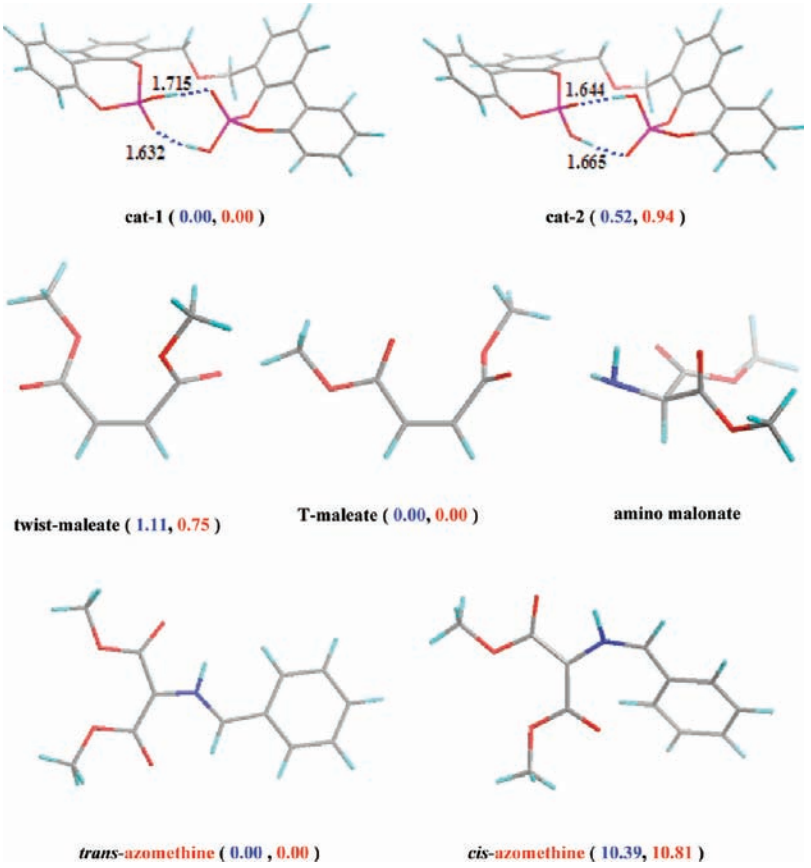

Figure 6. Calculated structures of catalyst, substrates and key intermediates with relative energies in enthalpy (blue) and Gibbs free energy (red) in kcal/mol and distance in angstrom.

To save computational time, the naphthyl moieties in the catalyst were replaced with phenyls and ethyl ester in the substrate with methyl ester.

The optimized structures of the catalyst, cat-1/2, and the substrates, amino-malonate and maleate, are shown in Figure 6. The BINOL-derived bisphosphoric acid cat-1/2 take on a half-moon shape with the two phosphoric acid groups forming two intramolecular hydrogen bonds (H-bonds). The calculated H-bond lengths are about 1.6−1.7 Å implying quite strong H-bonding interactions. This indicated that the linkage between the two BINOLs is proper for the two phosphoric acid groups to interact with each other. One of the two H-bonds formed on the inside of the half-moon shaped structure, and the other on the outside. The outside one should be easier to open and accept substrate to form the active complex by H-bonds. The inside one may play a proton-shuttle role to adjust the acidity and/or basicity of two phosphoric acid groups acting as a proton donor or acceptor in the reaction process.

The ester groups in the amino-malonate could assume various conformations. The most stable one, amino malonate, as shown in Figure 6, have the carbonyl oxygen atoms pointing toward the two hydrogen atoms of amine, respectively. The two ester groups in maleate prefer to a perpendicular orientation (T-shape) to avoid the repulsive interaction between the two carbonyl oxygen atoms. These structural features will be relevant to catalysis. In addition, there are two isomers for the key intermediate azomethine ylide, formed by condensation of amino-malonate with benzaldehyde. The two bulky groups of phenyl ring and diester

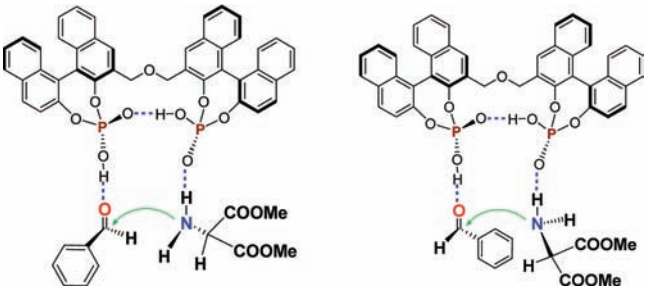

Figure 7. Proposed models of the nucleophilic addition of amino-malonate to benzadehyde.

methine may have *trans*- or *cis*- conformations. The *trans*-isomer was predicted to be more stable than the *cis*-isomer by about ca. ~10 kcal/mol. Consequently, the less stable *cis*-isomer is not considered in the following computations of 1,3-dipolar cycloaddition reactions.

The azomethine ylide is a key intermediate in this reaction. Hence, the formation of azomethine ylide was investigated in detail first. It was hypothesized that a BINOL-derived phosphoric acid catalyst can act simultaneously as an acid and a base to promote the reaction between an electrophile and a nucleophile. We thought the BINOL-derived bisphosphoric acid catalyst can play the same roles with additional proton-shuttling movement from the inside H-bond to adjust the acidity and basicity of both phosphoric acid groups. On the basis of the optimized

Scheme 1. Proposed Catalytic Cycle for the Formation of Azomethine Ylide

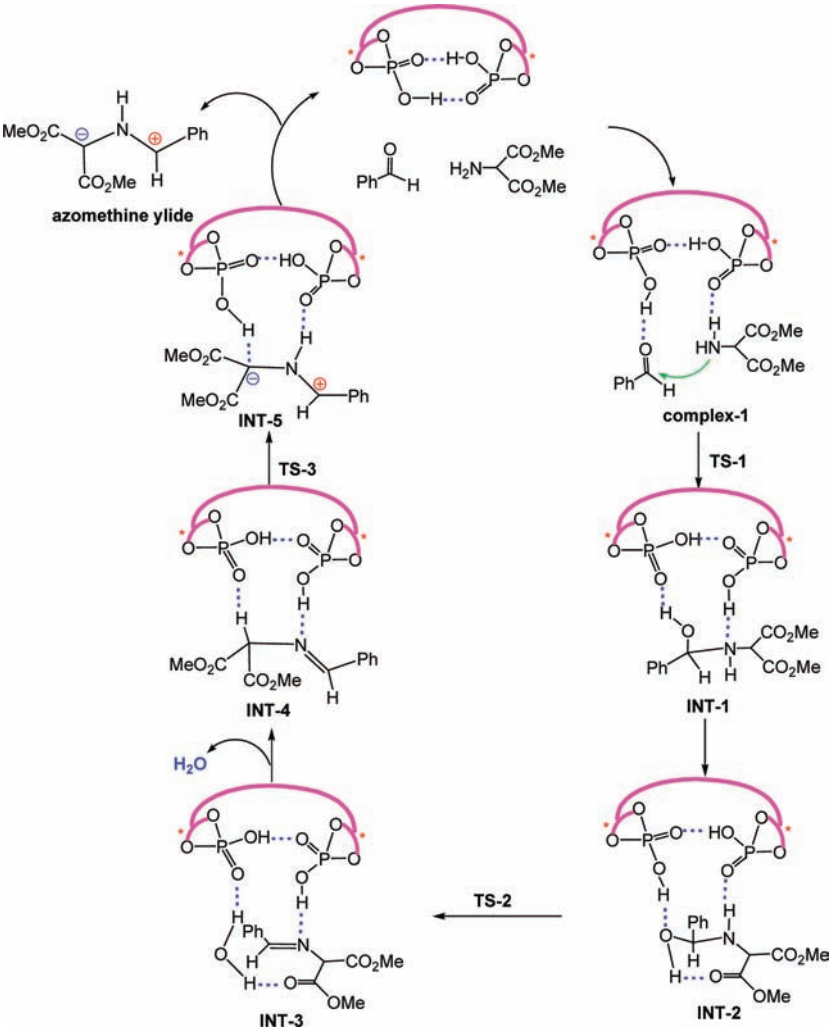

geometries of BINOL-derived bisphosphoric acids shown in Figure 6, we proposed a model for the nucleophilic addition of amino-malonate to benzaldehyde (Figure 7). According to this model, the outside, half-moon shaped, H-bond in the BINOL-derived bisphosphoric acid catalyst is opened when substrate approaches to release the phosphoric OH acid and P═O base. The phosphoric OH group acts as an acid to protonate the benzaldehyde, and the P═O group as a base to accept the amino-malonate. In both cases, H-bonding interaction is the intrinsic driving force. The inside H-bond may significantly improve the acidity and basicity simultaneously by proton shifting between the two phosphoric acid groups. The two substrates, benzaldehyde and amino-malonate, may approach backward or forward each other, respectively. The bulky groups of both substrates point in opposite direction and away from the BINOL-framework of the catalyst to reduce steric interactions. As such, there can be two possible complexes in which the catalyst can activate both reactants simultaneously to promote the nucleophilic addition of amine to carbonyl carbon. A proposed catalytic cycle for the formation of azomethine ylide is shown as Scheme 1.

The calculated results for the formation of azomethine ylide are shown in Figure 8. The formation of either complex, Complex-1-*R* or Complex-1-*S*, in Figure 8 was favorable with a binding energy of about −16.6 (ΔH) or 5.4 (ΔG) kcal/mol for Complex-1-*S*. The Complex-1-*S* was predicted to be more preferable than Complex-1-*R* about 2.7 (ΔH) or 1.86 (ΔG) kcal/mol. The subsequent location of transition state of the C−N bond forming step gave a similar prediction that TS-1-*S* was more stable than TS-1-*R* by about 2.7 (ΔH) or 1.9 (ΔG) kcal/mol. Again, the calculated results of the intermediate amino alcohol indicated also that INT-1-*S* was more stable than INT-1-*R* by about 2 kcal/mol. This predicted destabilization from Complex-1-*R* to INT-1-*R* may come from the pseudo 1,3-diaxial interaction between carbonyl oxygen atom and one ester group of amino-malonate. The calculated activation barrier for the C−N bond forming step was ∼6.49(ΔG) kcal/mol. This somewhat low activation barrier indicated that the catalyst is highly efficient and the proton shifting between the two phosphoric acids likely assisted in the nucleophilic addition process.

The next step is the dehydration of the amino alcohol intermediate, INT-1-*R*/*S*. The dehydration process can also be promoted by the BINOL-derived bisphosphoric acid catalyst. Proton transfer from the protonated amine of INT-1-*R*/*S* to protonated hydroxyl of INT-2-*R*/*S* gives the precursor of dehydration. The located complex structures are shown as INT-2-*R*/*S* in Figure 8. Such a perturbation is endergonic by ∼3 kcal/mol.

dx.doi.org/10.1021/ja204218h |*J. Am. Chem. Soc.* 2011, 133, 13504–13518

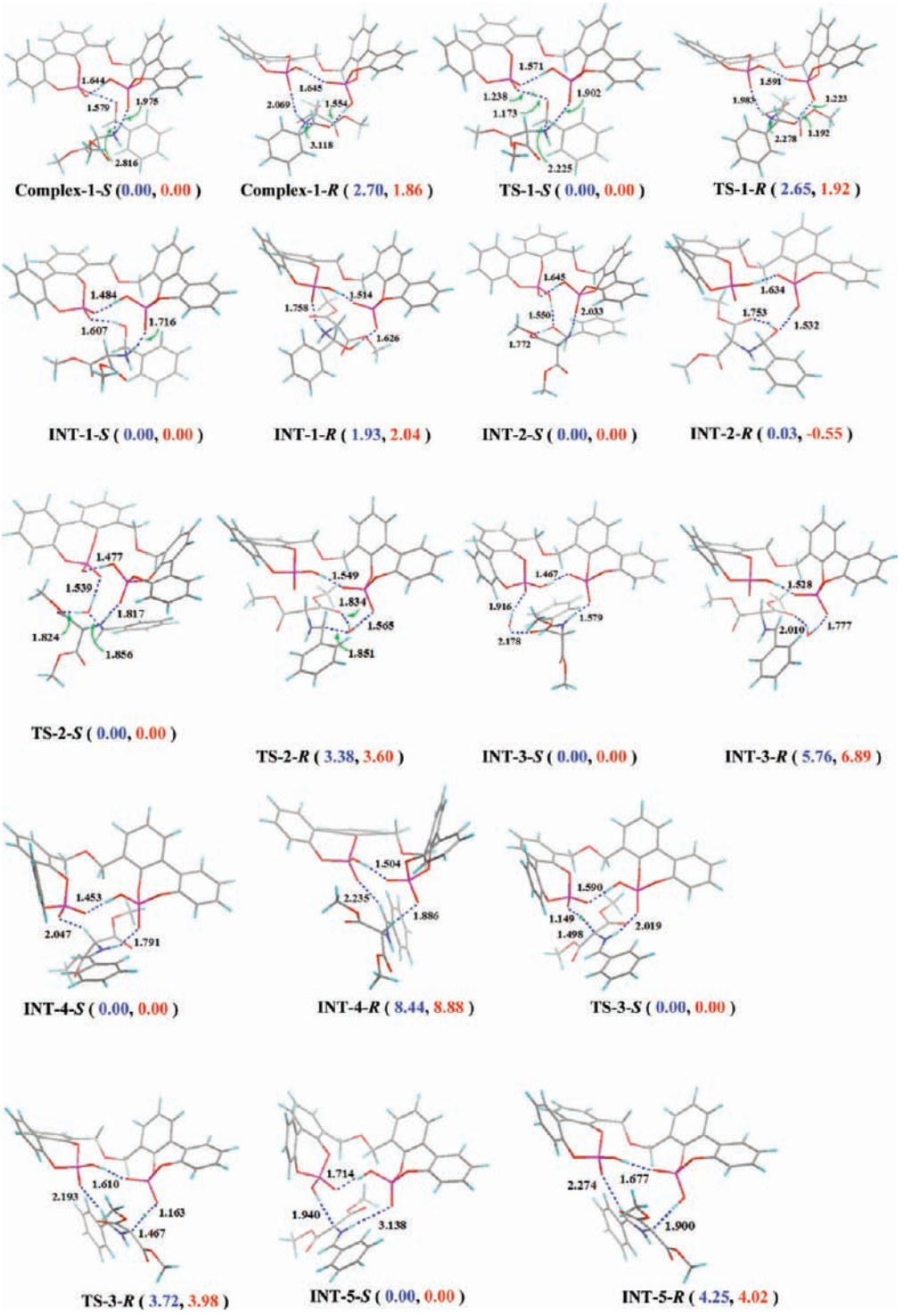

Figure 8. Located structures of complexes, transition states for the procedure of formation of azomethine ylide. Labeled distance in angstrom and relative energies in enthalpy (blue) and Gibbs free energy (red) in kcal/mol.

The located structure of intermediate INT-2-*R*/*S* indicated that the breakage of C−O bond may also be assisted by one of the ester groups by an intramolecular H-bonding interaction as shown in INT-2-*R*/*S*. These two structures were predicted to be of the same stability although the H−N was orientated in opposite directions in these two structures. The C−O bond breaking process can be promoted by the catalyst and the ester group, simultaneously. The located TSs were shown as TS-2-*R*/*S*, in which the hydroxyl leaving group is protonated by phosphoric acid and concurrently stabilized by an H-bonding interaction with one ester group. TS-2-*S* was predicted to be more favorable than TS-2-*R* by ∼3.5 kcal/mol due to the preferred H-bonds between H−N and phosphoryl oxygen in TS-2-*S*. The next complex of catalyst and protonated imine (intermediate

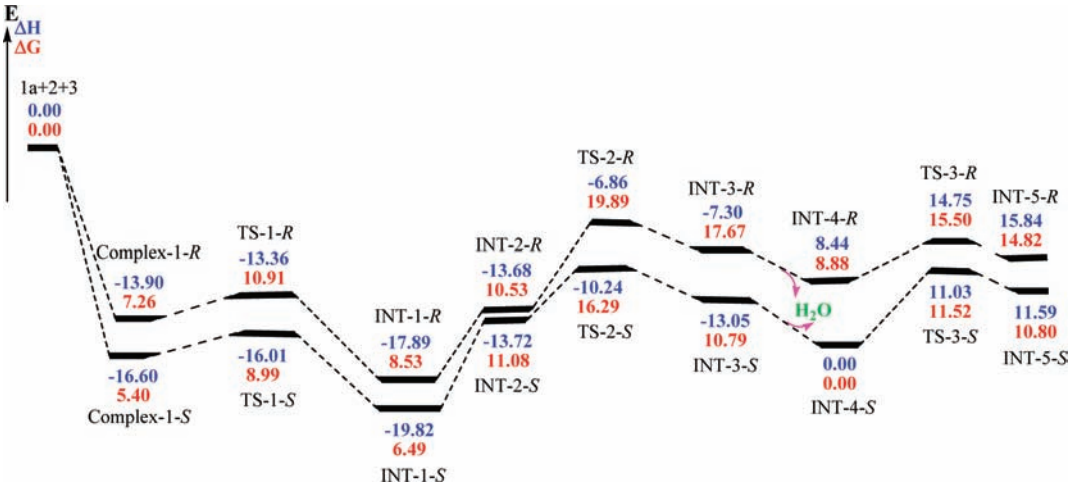

Figure 9. Energy profile for the formation of azomethine ylide.

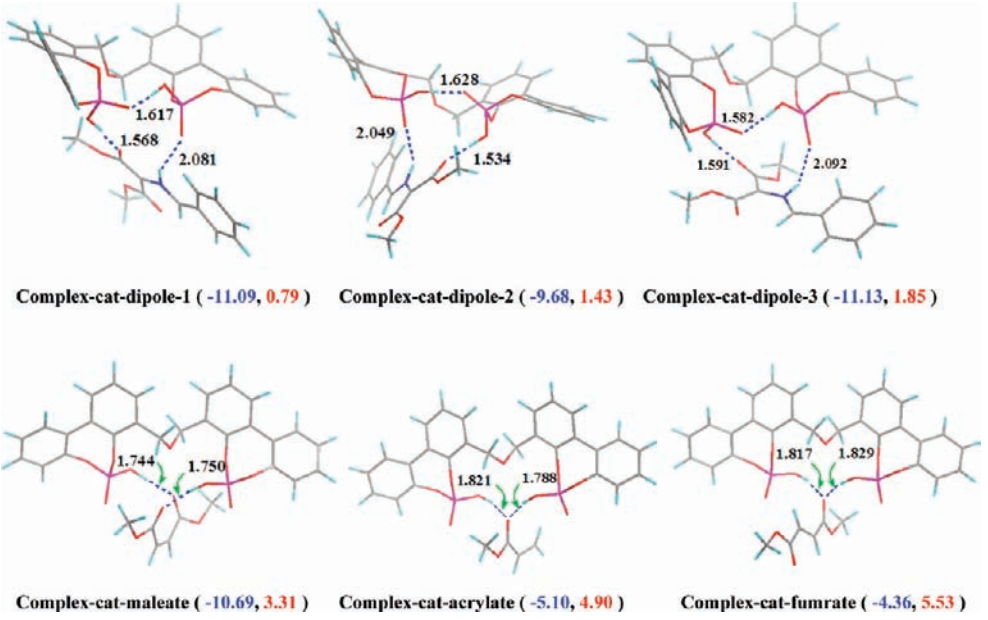

Figure 10. Located stable structures of complexes of catalyst with dipole and dipolarphiles, and binding energies in enthalpy (blue) and Gibbs free energy (red).

iminium) with H_2O was identified as INT-3-*R*/*S*. INT-3-*S* was predicted to be more stable than INT-3-*R* by about ~7 kcal/mol due to the lack of H-bonding interactions between H−N and phosphoryl oxygen in INT-3-*R*.

Release of the water molecule from the complex of INT-3-*R*/*S* and followed by a slight perturbation of the protonated imine, the precursor structure, for the formation of azomethine ylide were ascribed as INT-4-*R*/*S*. Similarly, INT-4-*R* was less stable than INT-4-*S* by about ~9 kcal/mol. The two phosphatic groups acted in concert now to promote the deprotonation of C−H to form azomethine ylide, one H-bonded H−N to stabilize the TS and the other one pointed to the H−C with one oxygen atom of the phosphate as a base to deprotonate the H of the H−C bond. The located TSs were shown as TS-3-*R*/*S*. Once again, TS-3-*S* was predicted to be more favorable than TS-3-*R* by about ~4 kcal/mol. After the shift of H of the H−C bond from iminum to phosphate, the catalyst was regenerated and the key intermediate azomethine ylide was produced. In the beginning of the formation of azomethine ylide, the formed complex between catalyst and azomethine ylide should take the orientation as INT-5-*R*/*S*, which were similar as those in the TS. The more stable complexes will be formed with a slight perturbation of the azomethine ylide, shown as complex-cat-dipole-1/2/3 in Figure 10, which were predicted to be more stable than INT-5-*R*/*S* by about 10 kcal/mol.

The energy profile for the formation of azomethine ylide from the nucleophilic addition reaction of amino-malonate to benzaldehyde, catalyzed by BINOL-derived bisphosphoric acid, is shown in Figure 9. The rate-determining step was predicted to be the elimination of H_2O, with an activation barrier of about 13 kcal/mol. It is lower compared to that in the formation of imine catalyzed by proline[25] or prolinamide.[26] This indicated bisphosphoric acid should be a more effective catalyst to promote the formation of imine.

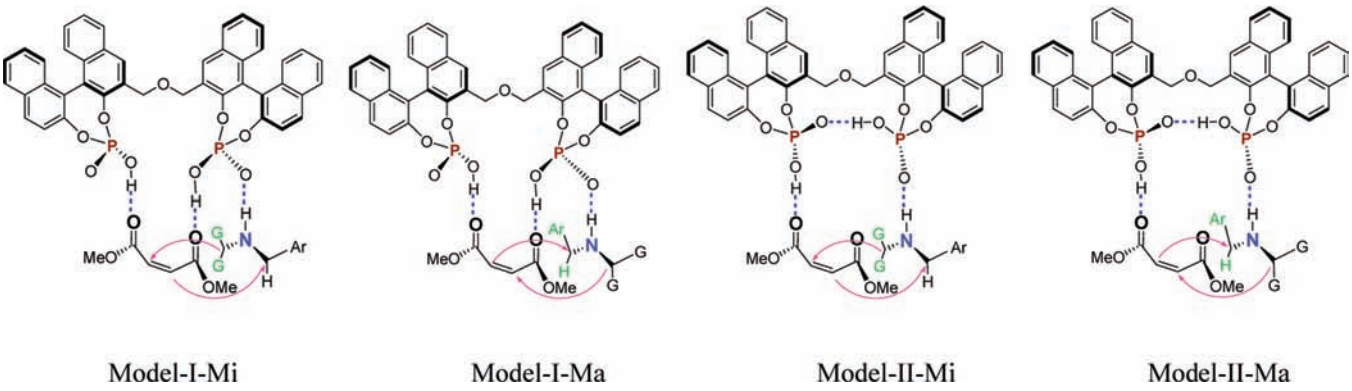

Figure 11. Proposed transition state models for the 1,3-dipolar cycloaddition reaction.

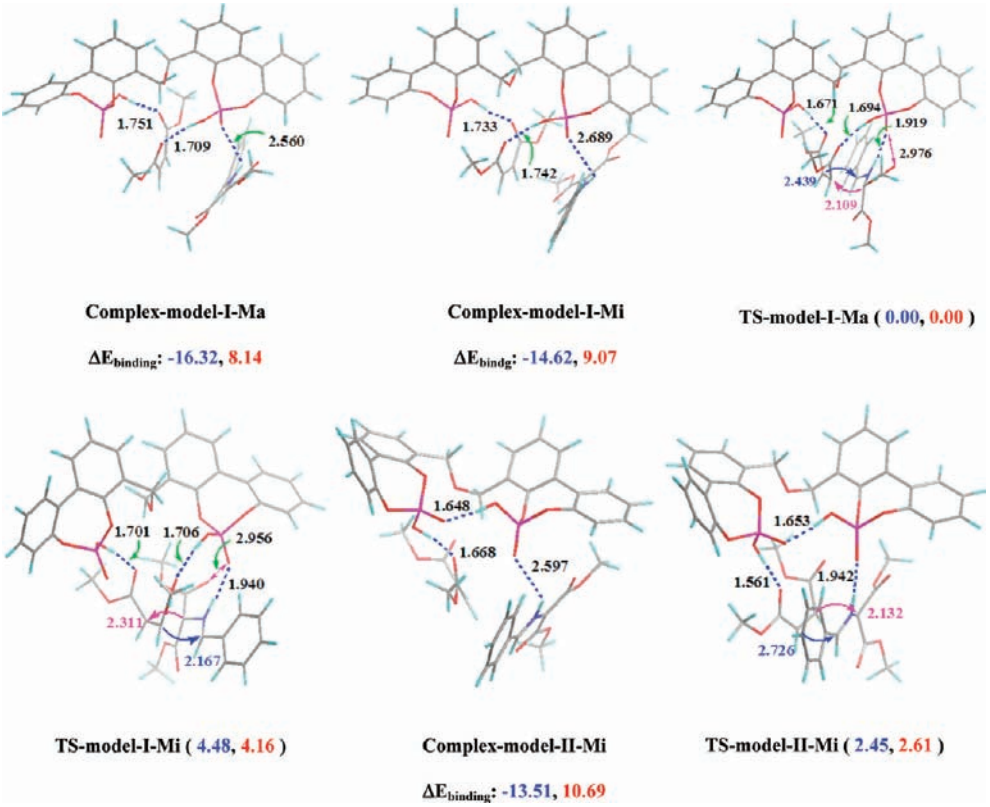

Figure 12. Located structures of complexes and TSs of 1,3-dipolar cycloaddition reaction of azomethine ylide with maleate.

The 1,3-dipolar cycloadditions of azomethine ylide with the electron deficient C═C bond of maleate, fumarate, and acrylate catalyzed by cat-2 were performed next, respectively. The high enantioselectivity observed experimentally for the 1,3-dipolar cycloaddition indicated a concerted process. The bisphosphoric acids may function similarly as in the process of formation of azomethine ylide. One phosphate acts as a base or H-bond acceptor to activate the 1,3-dipole, another as an acid or H-bond donor to make dipolarophile more electron deficient. The structures of the complexes between cat-2 and 1,3-dipole of azomethine ylide discussed previously as INT-5-*R*/*S* in Figure 8 and complex-cat-dipole-1/2/3, which correspond to other three different orientations of the dipole of azomethine ylide in the formed complex, are shown in Figure 10. The latter were predicted to be more favorable than the former ones by about 10 kcal/mol due to two better H-bond interactions between cat-2 and the dipole of the azomethine ylide. In complex-cat-dipole-3, the dipole and catalyst overlap. The *si*-face of the dipole was blocked by the catalyst completely. The dipolarophile approaches the dipole without interesting interaction with the catalyst. In complex-cat-dipole-1/2, the *si*-face of the dipole is opened and easily accessible for approach by the dipolarophile. In light of these structures, we located the complexes between cat-2 and different dipolarophiles. For maleate, the twisted *cis*-diester groups can approach bisphosphoric acid easily, and the cat-2 may open its double H-bonds to adopt the maleate by forming two new and stronger H-bonds, shown as complex-cat-maleate, with a C_2 axis, in Figure 10. The binding energy in enthalpy was predicted to be ~11 kcal/mol for complex-cat-maleate and is nearly the same as that of complex-cat-dipole-1.

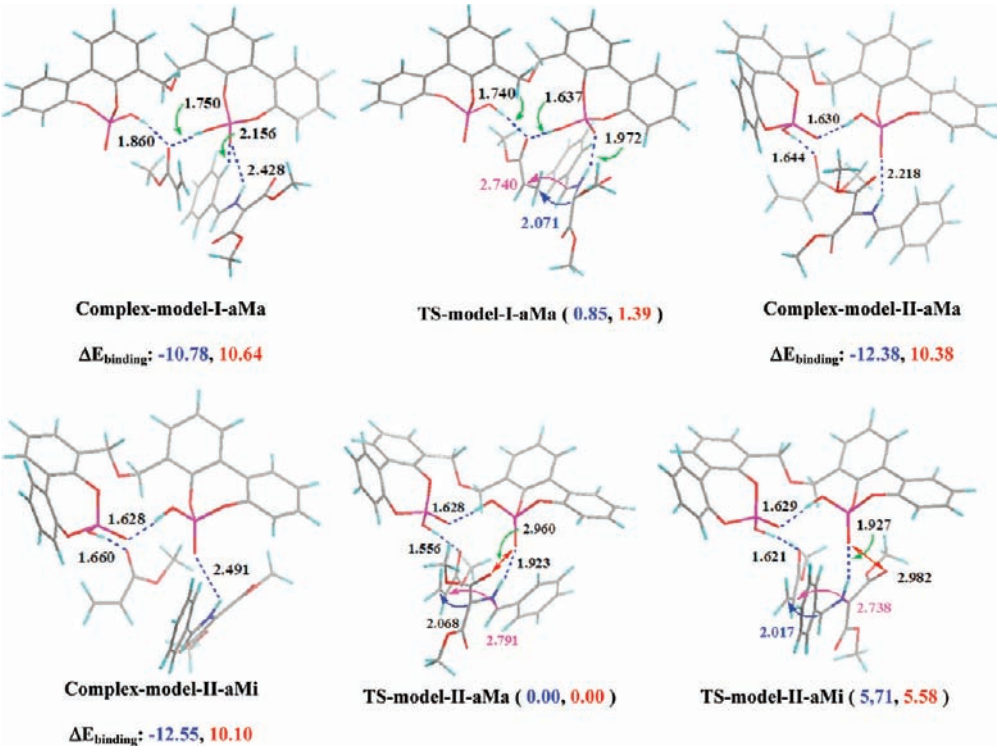

Figure 13. Located structures of complexes and TSs of 1,3-dipolar cycloaddition reaction of azomethine ylide with acrylate.

These high binding enthalpies indicated that there are strong interactions between the catalyst and both the dipole and the dipolarophile. Thus, a concerted 1,3-dipolar cycloaddition process could be promoted by the catalyst with both components binding with the catalyst simultaneously. Similarly, both fumarate and acrylate may form complexes with cat-2 by two H-bonds between the carbonyl oxygen of the ester and two OH groups of the catalyst as shown in Figure 10. However, the binding enthalpy was predicted to be about 5 kcal/mol, less than half of that of complex-cat-dipole and complex-cat-maleate.

In terms of the structural features of complex-cat-maleate and complex-cat-dipole-1, we propose two possible ways for the cycloaddition process, Model-I and Model-II, as shown in Figure 11. The structure of complex-cat-maleate has C_2 symmetry and the electron deficient dipolarphile maleate is highly activated by two H-bonds. The approach of the 1,3-dipole to maleate from either side is favorable. When the 1,3-dipole approaches maleate, the basic oxygen of phosphate may form an H-bond with H−N of the 1,3-dipole to direct its approaching and stabilizing the coming TS of the cycloaddition process shown as Model-I. On the basis of the structure of complex-cat-dipole-1, when maleate approaches 1,3-dipole, the OH of the phosphate may form an H-bond with the carbonyl oxygen of maleate to direct its approach and activate the dipolarophile as shown as Model-II. The *re*-facial approach of dipole to maleate was labeled as '-Ma', while the *si*-facial approach as '-Mi'.

The located complexes and TS structures are shown in Figure 12. Complex-model-I-Ma is more favorable than complex-model-I-Mi by about 2 kcal/mol. TS-model-I-Ma, which corresponds to the major product observed experimentally, was predicted to be more stable than TS-model-I-Mi by about 4 kcal/mol. The forming C−C bond distances were predicted to be 2.1−2.4 Å, indicating a concerted cycloaddition with a slight earlier nucleophilic attack of the electron rich carbon of the 1,3-dipole than the electron deficient one, with a difference of forming bond length of 0.33 Å in TS-model-I-Ma and 0.14 Å in TS-model-I-Mi. The selectivity possibly comes from the different interactions between the phosphate of cat-2 and the ester group of dipole. As shown in the TSs, the basic oxygen of the phosphate is pointing to its back. In TS-model-I-Ma, the ester group of the dipole was located in the front, so the basic oxygen of the ester was slightly away from the oxygen of the phosphate and close to the positively charged phosphorus atom. While in TS-model-I-Mi the ester group of the dipole was located in the back, and the basic oxygen of the ester was close to the oxygen of the phosphate and far away from the positively charged phosphorus atom. The repulsive interaction between the two basic oxygens and the attractive interaction between the basic oxygen and positively charged phosphorus atom, that is, the attractive ion pair that is interacting, made TS-model-I-Ma more favorable than TS-model-I-Mi, resulting in the observed stereoselectivity.

From the located structure of complex-cat-dipole-1 shown in Figure 10, the inside H-bond remains and the outside H-bond opens to the dipole to form two new H-bonds. Because one side of the dipole was blocked by the catalyst framework, the dipolarophile maleate could approach only from the *si*-face of the dipole to give the Model-II type cycloaddition. The located TS structure was shown as TS-model-II-Mi in Figure 12, which is the most stable one but not corresponding to the observed major product. In TS-model-II-Mi, the dipole interacted with the catalyst in the same way as in TS-model-I-Ma and TS-model-I-Mi. However, there is only one H-bond between the catalyst and maleate, so the maleate was less activated than that in TS-model-I-Ma and TS-model-I-Mi, and the TS-model-II-Mi was predicted to be less stable by about 2 kcal/mol than TS-model-I-Ma.

Substitution of one ester group of maleate with H atom gave the acrylate with similar 1,3-dipolar cycloaddition patterns as

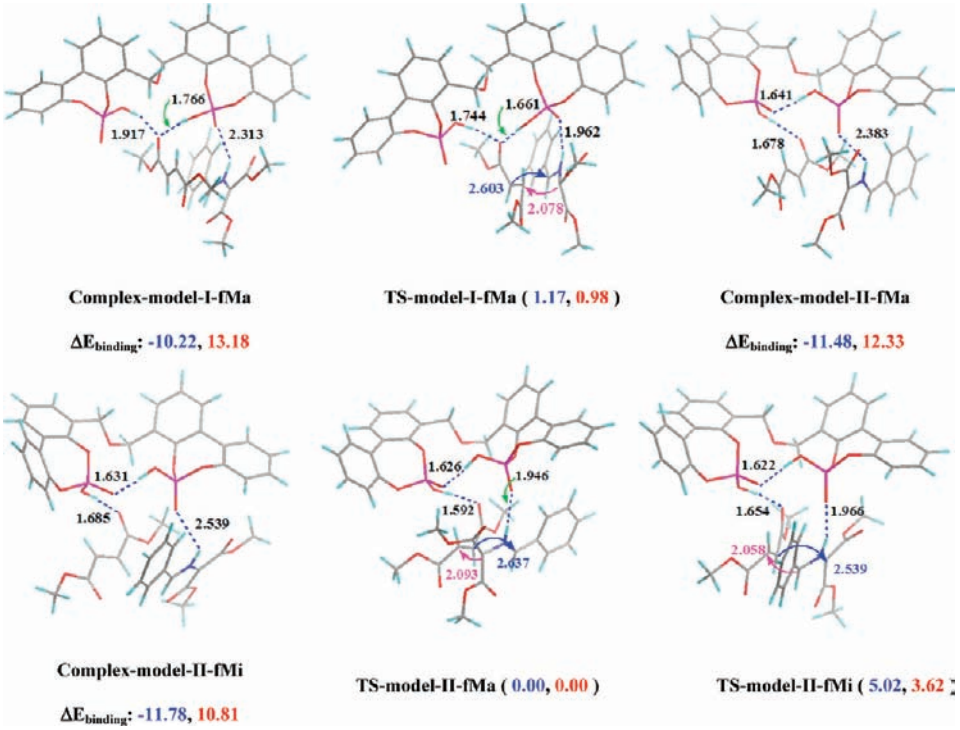

Figure 14. Located structures of complexes and TSs of 1,3-dipolar cycloaddition reaction of azomethine ylide with fumarate.

Model-I and Model-II in Figure 11. The located complex and TS structures were shown in Figure 13. Complex-model-II-aMa/aMi were predicted to be more favorable than complex-model-I-aMa by about 2 kcal/mol. The stability of the corresponding TSs was predicted with the same tendency as that of the complexes. TS-model-II-aMa, which afforded the observed major product, was more stable than TS-model-I-aMa by about 1 kcal/mol. This meant Model-II is slightly better than Model-I for the 1,3-cycloaddition of azomethine ylide with acrylate catalyzed by BINOL-derived bisphosphoric acid. In both TS-model-II-aMa and TS-model-I-aMa, the nucleophilic attack of the 1,3-dipole on the β-carbon of acrylate ocurs quite early with C−C distance of ~2.07 Å, compared to the other forming C−C bond distance of ~2.8 Å. Thus, the 1,3-dipolar cycloaddition reaction seemingly undergoes the Michael addition first, followed by an annulation to furnish the cycloadduct. However, the structure of the intermediate generated from the Michael addition could not be located, and therefore, the reaction may still proceed via a concerted rather than a sequential pathway. If the electron deficient carbon of the 1,3-dipole as nucleophile is added to α-carbon of acrylate, as in TS-model-II-aMi, the resulting TS has a higher activation barrier. TS-model-II-aMi was predicted to be less stable than TS-model-II-aMa by about 5.6 kcal/mol. In case of fumarate as the dipolarophile, similar calculated results were obtained. The located complex and TS structures were shown in Figure 14.

These computed results indicated that activating patterns in these reactions were different from maleate with two ester groups with a *cis*-configuration and for acrylate and fumarate with only one ester group in the dipolarophile. The two OH groups of two phosphoric acids in the catalyst may form two H-bonds with both ester groups of maleate, respectively, to make it more electron deficient and a much stronger dipolarophile to conduct a concerted 1,3-dipolar cycloaddition with azomethine ylide. However, for acrylate and fumarate, the ester groups may form one or two H-bonds with the catalyst as Model-I and Model-II to activate the α,β-C−C double bond. The calculated results suggest that the 1,3-dipolar cycloaddition reaction may proceed via a concerted rather than a sequential pathway although the attack on the β-carbon occurs quite earlier than that on the α-carbon of the activated ester by the nucleophilic center of the 1,3-dipole in both Model-I and Model-II, considering that the structure of the intermediate generated from the attack on the β-carbon could not be located. Moreover, the Model-II with one H-bond to the catalyst was slightly better than Model-I with two H-bonds for the nucleophilic attack on the β-carbon, implying that the one H-bonding interaction with the catalyst is sufficient to activate the acrylate and fumarate dipolarophiles, while the H-bond remaining in the catalyst may adjust the acidity and basicity of the two phosphate groups, simultaneously, by H-shifting between the two phosphate groups to activate the acceptor and donor appropriately. This BINOL-derived bisphosphoric acid may present a different activating model for substrates with various functional groups to facilitate different types of reaction with selectivity.

CONCLUSION

In summary, we have developed highly enantioselective 1,3-dipolar cycloaddition reactions using chiral bisphosphoric acids derived from binaphthols as catalysts. The linkage in bisphosphoric acids on the reaction were clarified as incorporation of an oxygen atom into the linker resulted in the best reactivity and enantioselectivity. This organocatalytic 1,3-dipolar cycloaddition reaction by catalyst **1a** is applicable to a wide range of azomethine ylides derived from various aldehydes and α-amino esters with electron-deficient dipolarophiles, providing a highly enantioselective method to access structurally diverse pyrrolidines with

excellent optical purity. Theoretical calculations with the DFT method indicated that the bisphosphoric acids catalyst **1a** may take on a half-moon shape with the two phosphoric acid groups forming two intramolecular hydrogen bonds. It may take two models to promote reaction: two H-bonds are opened to activate electrophile by its two hydroxyls with two H-bonding interactions simultaneously or only one H-bond is opened and the another one remains to play a proton-shuttle role to adjust the acidity and/or basicity of two phosphoric acid groups acting as a proton donor or acceptor in the reaction process. Computation on the formation of key intermediate azomethine ylide and the transition states of the 1,3-dipolar cycloaddition step showed that the neucleophile and electrophile were simultaneously activated by the bifunctional chiral bisphosphoric acids through formation of hydrogen bonds. The effect of the bisphosphoric acids on the reactivity and stereochemistry of three-component 1,3-dipolar cycloaddition reaction was also theoretically rationalized. For the 1,3-dipolar cycloaddition reaction of azomethine ylide with maleate, the two H-bonds of catalyst were opened to accept maleate by its two hydroxyls forming two new H-bonds to activate the electron-deficient C−C double bound. The ion pair interaction between the phosphate of catalyst and the ester of azomethine ylide accounted for the high stereoselectivity for this 1,3-dipolar cycloaddition reaction. For the dipolarophile, acrylate or fumarate derivatives, one H-bond in catalyst remains to adjust the acidity and basicity of two phosphoric acids to activate the dipole and dipolarophile more effectively. These procedures provide new accesses to a wide spectrum of structurally diverse pyrrolidines and their potentially pharmaceutical relevant derivatives with high enantiomeric purity.

■ ASSOCIATED CONTENT

Supporting Information. Experimental details, characterization of new compounds, selected NMR and HPLC spectra, and complete ref 24. This material is available free of charge via the Internet at http://pubs.acs.org.

■ AUTHOR INFORMATION

Corresponding Author
gonglz@ustc.edu.cn; luosw@ustc.edu.cn

■ ACKNOWLEDGMENT

We are grateful for financial support from NSFC (20732006, 21072181), MOST (973 program 2009CB825300), Ministry of Education, and CAS. We also thank Dr. Fei Liu in Australia for polishing English and professor Terada (Tohoku University in Japan) for donating extra pure silica gel (Merck).

■ REFERENCES

(1) Schreiber, S. L. *Science* **2000**, *287*, 1964.

(2) For reviews: Pearson, W. H. In *Studies in Natural Product Chemistry*; Atta-Ur-Rahman, Ed.; Elsevier: New York, 1998; Vol. 1, p 323.

(3) For reviews:(a) Sardina, F. J.; Rapoport, H. *Chem. Rev.* **1996**, *96*, 1825. (b) Coldham, I.; Hufton, R. *Chem. Rev.* **2005**, *105*, 2765. (c) Pandey, G.; Banerjee, P.; Gadre, S. R. *Chem. Rev.* **2006**, *106*, 4484. (d) Nair, V.; Suja, T. D. *Tetrahedron* **2007**, *63*, 12247. (e) For highlights, see: Nájera, C.; Sansano, J. M. *Angew. Chem., Int. Ed.* **2005**, *44*, 6272.

(4) (a) Padwa, A.; Chen, Y.-Y.; Chlacchio, U.; Dent, W. *Tetrahedron* **1985**, *41*, 3529. (b) Deprez, P.; Rouden, J.; Chiaroni, A.; Riche, C.; Royer, J.; Husson, H.-P. *Tetrahedron Lett.* **1991**, *32*, 7531. (c) Anslow, A. S.; Harwood, L. M.; Lilley, I. A. *Tetrahedron: Asymmetry* **1995**, *6*, 2465. (d) Garner, P.; Ho, W. B.; Shin, H. *J. Am. Chem. Soc.* **1993**, *115*, 10742. (e) Garner, P.; Dogan, O. *J. Org. Chem.* **1994**, *59*, 4. (f) Takano, S.; Moriya, M.; Ogasawara, K. *Tetrahedron: Asymmetry* **1992**, *3*, 681. (g) Wee, A. G. H. *J. Chem. Soc., Perkin. Trans. 1* **1989**, 1363. (h) Nájera, C.; Gracia, R. M. D.; Sansano, J. M. *Tetrahedron: Asymmetry* **2006**, *17*, 1985. (i) Nájera, C.; Gracia, R. M. D.; Sansano, J. M.; Cossio, F. P. *Eur. J. Org. Chem.* **2007**, 5038.

(5) (a) Allway, P.; Grigg, R. *Tetrahedron Lett.* **1991**, *32*, 5817. (b) Grigg, R. *Tetrahedron: Asymmetry* **1995**, *6*, 2475.

(6) (a) Longmire, J. M.; Wang, B.; Zhang, X. *J. Am. Chem. Soc.* **2002**, *124*, 13400. (b) Gothelf, A. S.; Gothelf, K. V.; Hazell, R. G.; Jørgensen, K. A. *Angew. Chem., Int. Ed.* **2002**, *41*, 4236.

(7) (a) Chen, C.; Li, X.; Schreiber, S. L. *J. Am. Chem. Soc.* **2003**, *125*, 10174. (b) Knöpfel, T. F.; Aschwanden, P.; Ichikawa, T.; Watanabe, T.; Carreira, E. M. *Angew. Chem., Int. Ed.* **2004**, *43*, 5971. (c) Cabrera, S.; Arrayás, R. G.; Carretero, J. C. *J. Am. Chem. Soc.* **2005**, *127*, 16394. (d) Yan, X.-X.; Peng, Q.; Zhang, Y.; Zhang, K.; Hong, W.; Hou, X.-L.; Wu, Y.-D. *Angew. Chem., Int. Ed.* **2006**, *45*, 1979. (e) Zeng, W.; Chen, G.-Y.; Zhou, Y.-G.; Li, Y.-X. *J. Am. Chem. Soc.* **2007**, *129*, 750. (f) Saito, S.; Tsubogo, T.; Kobayashi, S. *J. Am. Chem. Soc.* **2007**, *129*, 5364. (g) Tsubogo, T.; Saito, S.; Seki, K.; Yamashita, Y.; Kobayashi, S. *J. Am. Chem. Soc.* **2008**, *130*, 13321. (h) Wang, C.-J.; Liang, G.; Xue, Z.-Y.; Gao, F. *J. Am. Chem. Soc.* **2008**, *130*, 17250. (i) Arai, T.; Mishiro, A.; Yokoyama, N.; Suzuki, K.; Sato, H. *J. Am. Chem. Soc.* **2010**, *132*, 5338. (j) Padilla, S.; Tejero, R.; Adrio, J.; Carretero, J. C. *Org. Lett.* **2010**, *12*, 5608. (k) Zhang, C.; Yu, S.-B.; Hu, X.-P.; Wang, D.-Y.; Zheng, Z. *Org. Lett.* **2010**, *12*, 5542. (l) Yamashita, Y.; Guo, X.-X.; Takashita, R.; Kobayashi, S. *J. Am. Chem. Soc.* **2010**, *132*, 3262. (m) Oura, I.; Shimizu, K.; Ogata, K.; Fukuzawa, S. *Org. Lett.* **2010**, *12*, 1752. (n) Rocío, R. M.; María, G. E.; Adrio, J.; Carretero, J. C. *J. Org. Chem.* **2010**, *75*, 233. (o) Rocío, R. M.; Alonso, I.; Adrio, J.; Carretero, J. C. *Chem.—Eur. J.* **2010**, *16*, 5286.

(8) Kudryavtsev, K. V.; Zagulyaeva, A. A. *Russ. J. Org. Chem.* **2008**, *44*, 378.

(9) (a) Vicario, J. L.; Reboredo, S.; Badía, D.; Carrillo, L. *Angew. Chem., Int. Ed.* **2007**, *46*, 5168. (b) Ibrahem, I.; Rios, R.; Vesely, J.; Cordova, A. *Tetrahedron. Lett.* **2007**, *48*, 6252. For a leading literature on LUMO lowering by Iminium: (c) Jen, W. S.; Wiener, J. J. M.; MacMillan, D. W. C. *J. Am. Chem. Soc.* **2000**, *122*, 9874.

(10) (a) Xue, M.-X.; Zhang, X.-M.; Gong, L.-Z. *Synlett* **2008**, 691. (b) Liu, Y.-K.; Liu, H.; Du, W.; Yue, L.; Chen, Y.-C. *Chem.—Eur. J.* **2008**, *14*, 9873.

(11) Jiao, P.; Nakashima, D.; Yamamoto, H. *Angew. Chem., Int. Ed.* **2008**, *47*, 2411.

(12) For the preliminary report, see:Chen, X.-H.; Zhang, W.-Q.; Gong, L.-Z. *J. Am. Chem. Soc.* **2008**, *130*, 5652.

(13) For reviews:(a) Akiyama, T. *Chem. Rev.* **2007**, *107*, 5744. (b) Doyle, A. G.; Jacobsen, E. N. *Chem. Rev.* **2007**, *107*, 5713. (c) Terada, M. *Chem. Commun.* **2008**, 4097. (d) Terada, M. *Synthesis* **2010**, *12*, 1929. For leading references: (e) Uraguchi, D.; Terada, M. *J. Am. Chem. Soc.* **2004**, *126*, 5356. (f) Akiyama, T.; Itoh, J.; Yokota, K.; Fuchibe, K. *Angew. Chem., Int. Ed.* **2004**, *43*, 1566. For recent examples not included in reviews: (g) Jain, P.; Antilla, J. C. *J. Am. Chem. Soc.* **2010**, *132*, 11884. (h) Husmann, R.; Sugiono, E.; Mersmann, S.; Raabe, G.; Rueping, M.; Bolm, C. *Org. Lett.* **2011**, *13*, 1044. (i) Rueping, M.; Brinkmann, C.; Antonchick, A. P.; Atodiresei, I. *Org. Lett.* **2010**, *12*, 4604. (j) Čorić, I.; Müller, S.; List, B. *J. Am. Chem. Soc.* **2010**, *132*, 17370. (k) Lu, G.-J.; Birman, V. B. *Org. Lett.* **2011**, *13*, 356.

(14) Yu, J.; He, L.; Chen, X.-H.; Song, J.; Chen, W.-J.; Gong, L.-Z. *Org. Lett.* **2009**, *11*, 4946.

(15) Chen, X.-H.; Wei, Q.; Luo, S.-W.; Xiao, H.; Gong, L.-Z. *J. Am. Chem. Soc.* **2009**, *131*, 13819.

(16) (a) Matsunaga, S.; Das, J.; Roels, J.; Vogl, E. M.; Yamamoto, N.; Iida, T.; Yamaguchi, K.; Shibasaki, M. *J. Am. Chem. Soc.* **2000**, *122*, 2252. (b) Majima, K.; Takita, R.; Okada, R.; Ohshima, T.; Shibasaki, M. *J. Am. Chem. Soc.* **2003**, *125*, 15837. (c) Kumagai, N.; Matsunnga, S.; Kinoshita, T.; Harada, S.; Okada, S.; Sakamoto, S.; Yamaguchi, K.; Shibasaki, M.

J. Am. Chem. Soc. **2003**, *125*, 2169. (d) Vogl, E. M.; Matsunaga, S.; Kanai, M.; Iida, T.; Shibasaki, M. *Tetrahedron Lett.* **1998**, *39*, 7917.

(17) (a) Kurihara, K.; Yamamoto, Y.; Miyaura, N. *Adv. Synth. Catal.* **2009**, *351*, 260. (b) Robinson, J. E.; Taylor, R. J. K. *Chem. Commun.* **2007**, 1617.

(18) We also evaluated the reaction catalyzed by calcium salt of **1a**, but no reaction occurred. Moreover, ICP-OES analysis indicated trace amount of metals (see Supporting Information). The results sufficiently rule out the effect of metal contamination on the stereoselectivity, which has been found in other reactions: (a) Hatano, M.; Moriyama, K.; Maki, T.; Ishihara, K. *Angew. Chem., Int. Ed.* **2010**, *49*, 3823. (b) Klussmann, M.; Ratjen, L.; Hoffmann, S.; Wakchaure, V.; Goddard, R.; List, B. *Synlett* **2010**, 2189. (c) Terada, M.; Kanomata, K. *Synlett* **2011**, 1255.

(19) (a) Gao, W. Z.; Zhang, X. M.; Raghunath, M. *Org. Lett.* **2005**, *7*, 4241. (b) Alemparte, C.; Blay, G.; Jørgensen, K. A. *Org. Lett.* **2005**, *7*, 4569. (c) Nájera, C.; Retamosa, M. G.; Sansano, J. M. *Angew. Chem., Int. Ed.* **2008**, *47*, 6055. (d) Kim, H. Y.; Shih, H. J.; Knabe, W. E.; Oh, K. *Angew.Chem., Int. Ed.* **2009**, *48*, 7420.

(20) For more examples, see:Cheng, M.-N.; Wang, H.; Gong, L.-Z. *Org. Lett.* **2011**, *13*, 2418.

(21) (a) Akiyama, T.; Morita, H.; Itoh, J.; Fuchibe, K. *Org. Lett.* **2005**, *7*, 2583. (b) Yamanaka, M.; Itoh, J.; Fuchibe, K.; Akiyama, T. *J. Am. Chem. Soc.* **2007**, *129*, 6756. (c) Akiyama, T.; Morita, H.; Bachu, P.; Mori, K.; Yamanaka, M.; Hirata, T. *Tetrahedron.* **2009**, *65*, 4950. (d) Gridnev, I. D.; Kouchi, M.; Sorimachi, K.; Terada, M. *Tetrahedron Lett.* **2007**, *48*, 497. (e) Simon, L.; Goodman, J. M. *J. Am. Chem. Soc.* **2008**, *130*, 8741. (f) Simon, L.; Goodman, J. M. *J. Am. Chem. Soc.* **2009**, *131*, 4070. (g) Simon, L.; Goodman, J. M. *J. Org. Chem.* **2010**, *75*, 589. (h) Marcelli, T.; Hammar, P.; Himo, F. *Chem.—Eur. J.* **2008**, *14*, 8562. (i) Marcelli, T.; Hammar, P.; Himo, F. *Adv. Synth. Catal.* **2009**, *351*, 525. (j) Yamanaka, M.; Hirata, T. *J. Org. Chem.* **2009**, *74*, 3266. (k) Shi, F.-Q.; Song, B.-A. *Org. Biomol. Chem.* **2009**, *7*, 1292.

(22) Backe, A. D. *J. Chem. Phys.* **1983**, *98*, 5648.

(23) Gill, P. M. W.; Johnson, B. G.; Pople, J. A.; Frisch, M. J. *Chem. Phys. Lett.* **1992**, *197*, 499.

(24) Frisch, M. J., et al. *Gaussian 03*, Revision D.03; Gaussian, Inc.: Wallingford, CT, 2004.

(25) Bahmanyar, S.; Houk, K. N. *J. Am. Chem. Soc.* **2001**, *123*, 11273.

(26) Rao, Q.-Q.; Luo, S.-W.; Gong, L.-Z. *Chin. Sci. Bull.* **2010**, *55*, 1742.